Effect of demyelination on diffusion tensor indices: a Monte Carlo simulation study

Maximilian Pietsch[1] and J-Donald Tournier[1]
[1]*Centre for the Developing Brain, King's College London, London, London, United Kingdom*

TARGET AUDIENCE – Researchers interested in analysing and modelling diffusion in demyelinating diseases.

PURPOSE – Diffusion tensor imaging (DTI) of white matter MRI data is widely used to investigate myelin loss, remyelination and axonal integrity of white matter in demyelinating diseases such as multiple sclerosis (MS)[1]. Increase in the diffusion coefficient perpendicular to the white matter tracts (radial diffusivity D_r) is frequently associated with damage to myelin, and the fractional anisotropy (FA) is often interpreted as a measure of axonal integrity[2]. However, lesions in MS show a variety of diffusion characteristics depending on the physiological processes accompanying the demyelination, such as axonal disruption, swelling and loss, white matter tract atrophy (and any combination of them) with different types of progression of the disease, which complicates the interpretation of diffusion data. Lesions in acute relapsing-remitting MS, for instance, typically show an increase in diffusion which is associated with the presence of edema, although the opposite behaviour has also been reported[3]. In this study, we performed Monte Carlo (MC) simulations to investigate the effect of demyelination on DTI-based measures with randomized axon arrangements, to provide insights into the interpretation of these measures in the context of demyelination.

METHODS – We simulated axons whose distribution of inner diameters was modelled as a gamma distribution fitted to histological data of the human uncinate/inferior occipitofrontal fascicle[4]. The g-ratio, defined as the fraction of the inner to outer axonal diameters, was fitted (r^2=0.975) to macaque myelin sheath measurements also from [4]. We used the resulting g-ratio of 0.75 for healthy tissue as a lower bound and increased it up to a g-ratio of one (complete loss of myelin) in four steps. Axon arrangements were simulated with periodic boundaries following the algorithm from [5] over a range of axonal packing densities (by surface area) from 0.54 to 0.81 as shown in Fig 1. The demyelination was modelled in two ways: holding inner axonal radii constant with (a) fixed axon locations (top row in Fig. 1) or (b) demyelination with fibre tract contraction so that the extra-cellular volume fraction stays constant (bottom row). In both cases, the contribution of the myelin sheath to the signal was ignored; this approximation is estimated to introduce errors smaller than 8% or 4.5% for b=1000s/mm^2 or b=3000s/mm^2, respectively ($T_{2,myelin}$=26ms, $T_{2,cellular}$=80ms, assuming 10% to 30% proton density in myelin[6], Stejskal Tanner sequence: Δ_{1000}=30ms, Δ_{3000}=42.8ms, δ_{1000}=20.7ms, δ_{3000}=30ms). Also supporting this assumption is that the observed diffusion tensor in-vivo is independent of the myelin water fraction[7]. All MC-simulations and non-linear tensor fits were performed with the Camino toolkit[8] for 61 gradient directions and both b-values independently with equal particle densities and diffusion constants ($2x10^{-9}m^2s^{-1}$) in the intra- and extra-cellular compartments. The calibration of the number of particles (N) and time steps (t) used in the MC-simulation was performed as described in [5] and yielded N=10000 and t=1000 for standard deviations of the normalized signal smaller than 1% for 20 repeated measurements.

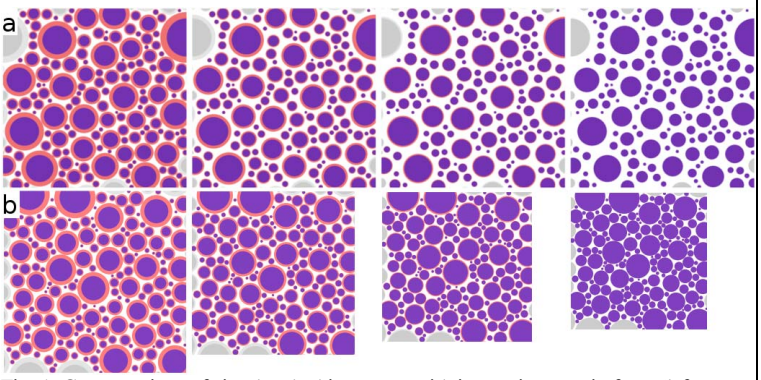

Fig. 1: Cross sections of simulated white matter with increasing g-ratio from (left to right). Myelin is shown in red, axons in purple. Light grey circles correspond to clones for periodic boundaries. Demyelination with a) increased extracellular volume fraction, b) constant extracellular volume fraction. Top row box side length: 15µm

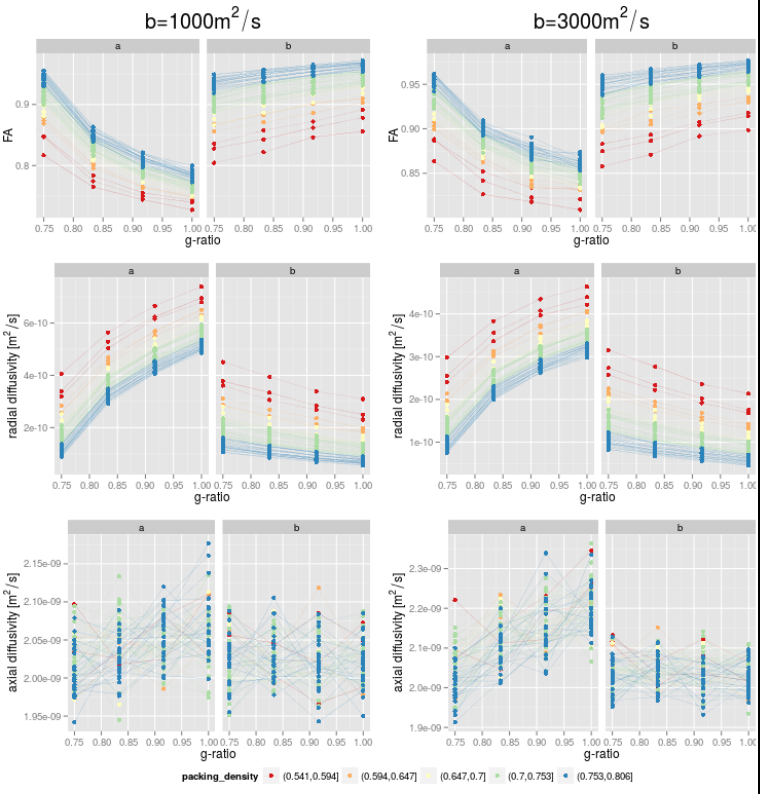

Fig. 2 Fractional anisotropy (FA) and radial and axial diffusivity plotted against g-ratio for both simulation scenarios with b=1000s/mm^2 and b=3000s/mm^2. Data originating from the same original axon arrangement are linked with lines. Warm to cold colours: Increasing initial axonal packing density (1- extracellular volume fraction).

RESULTS – The simulations where the extra-cellular volume fraction was increased with increasing g-ratio (a) showed a relative increase in radial diffusivity with complete myelin loss by a factor of approximately 3 for b=1000s/mm^2 and 2 for b=3000s/mm^2 (Fig. 2, middle row). These tendencies are reversed with simulation settings (b) where the extra-cellular volume fraction remains unchanged, showing decreased radial diffusivity with increasing g-ratio.

DISCUSSION – Demyelination was simulated in the ideal case of parallel cylinders without crossing fibres, which would otherwise render the neuro-biological interpretation of D_r and FA questionable[9]. Our simulations show that the apparent radial diffusivity depends on the packing density as well as the g-ratio. More importantly, the radial diffusivity can increase or decrease with demyelination depending on how the extra-cellular space behaves. When the intra-axonal volume remains unchanged, the increased extra-cellular space causes an increase in radial diffusivity, as has been previously reported. However, if the axons increase in density to use up the additional space (as might happen in chronic demyelination, or indeed in healthy unmyelinated white matter), radial diffusivity can go down, with a corresponding increase in FA. This suggests that the interpretation of D_r as a marker of demyelination is at best questionable, even in single fibre regions. Likewise, the interpretation of FA as a marker of axonal integrity is also problematic, even without the well-known confounding effects of crossing fibres.

REFERENCES – 1. Fox, R.J. et al. AJNR Am J Neuroradiol 32:85–91, doi:10.3174/ajnr.A2238 (2011) **2.** Song, S.K. et al. Neuroimage, 20:1714–22 (2003) **3.** Balashov, K., & Lindzen, E., Multiple Sclerosis Journal, 18(12), 1745–1753. doi:10.1177/1352458512445407 (2012). **4.** Liewald, D. et al. Biological Cybernetics, doi:10.1007/s00422-014-0626-2 (2014) **5.** Hall, M. G., & Alexander, D. C. IEEE Transactions on Medical Imaging, 28(9), 1354–1364 (2009) **6.** Dean Douglas C, NeuroImage, 84, 742–752 (2014) **7.** Borich, M.R., NeuroImage: Clinical, Volume 2, 569–580 (2013) **8.** Cock P.A. et al. Proc. Proc. Intl. Soc. Mag. Reson. Med. 14 (2006) **9.** Wheeler Kingshott, C. A. M., & Cercignani, M. Magnetic Resonance in Medicine, 61(5), 1255–1260 (2009)

ACKNOWLEDGEMENT – We would like to thank the MRC strategic funds and GSTT BRC.